

## Proton - Electron discrimination with the AMS02 Electromagnetic Calorimeter

L. BASARA<sup>1</sup>, FOR THE AMS02 COLLABORATION.

<sup>1</sup> LAPP IN2P3-CNRS and Université de Savoie, 74940 Annecy-le-Vieux, France

basara@lapp.in2p3.fr

**Abstract:** The 3D imaging calorimeter of AMS was designed to precisely reconstruct the longitudinal and lateral profiles of the shower and to measure the energy of electromagnetic particles. The longitudinal and lateral segmentation of the calorimeter, combined with the measurement of the particle energy loss, allow for a very high discriminating power between electromagnetic and hadronic showers, necessary to beat down the dominant proton background in the electron/positron signal. To reach the required rejection power, a multivariate technique has been developed which makes use of both flight data and Monte Carlo simulation to build several estimators. A description of the technique, together with its performance in background rejection as a function of the measured energy and of the signal efficiency will be given.

**Keywords:** icrc2013, AMS-02, calorimeter, proton rejection

### 1 Introduction

Installed on the ISS, AMS-02 is a general purpose particle detector capable of identifying all cosmic ray species: photons, electrons, protons and nuclei as well as all corresponding anti-particles [1].

AMS-02 will measure spectra for nuclei in the energy range from 0.5 GeV/nucl to 2 TeV/nucl with 1% accuracy. The scientific goals of AMS are to reach for antimatter search a sensitivity of of  $1 \times 10^{-10}$  (ratio of anti-helium to helium), an  $e^+/p$  rejection of  $1 \times 10^6$  and to measure the composition and spectra of charged particles with an accuracy of 1%. Confirming the previous measurements by AMS-01, HEAT, PAMELA and Fermi, AMS02 has extended the energy domain up to 300 GeV and precisely measured the  $e^+/(e^+ + e^-)$  ratio. A large deviation with respect to the model expectations is observed.

The cosmic rays are mainly composed of protons, a background to get rid of in order to measure the positron fraction. We present the method implemented in AMS-02 to take care of the background and estimate what is left after the selections.

### 2 The detector

AMS-02 is a general purpose detector to study primordial cosmic ray particles in the energy range from 0.5 to 2000 GeV. It consists of six complementary sub-detectors, providing measurements of the energy, the mass and the charge leading to an unambiguous identification of the cosmic rays. Its general layout is presented in Figure 1.

The six subdetectors are :

- a Transition Radiation Detector participating to the  $e/p$  rejection and to the charge measurement via  $dE/dX$ ;
- four planes of Time of Flight counters, the key detector for the trigger on charged particles and the measure of the timing, velocity and charge via  $dE/dX$ ;
- a Permanent Magnet of 0.14 T important to determine the sign of the charge combined with a precision

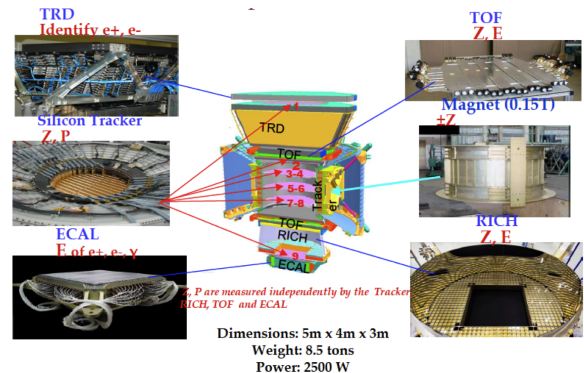


**Fig. 1:** The AMS layout with the different subdetectors.

silicon Tracker consisting of 9 layers, out of which 7 are in the magnetic field (Inner tracker). This detector provides the rigidity and the charge via  $dE/dX$  measurements and participates to the  $e/p$  rejection by comparing the rigidity with the energy measured in the calorimeter;

- an array of Veto Counters included in the trigger system, surrounding the Tracker;
- a Ring Imaging Cherenkov detector providing charge and velocity measurements
- an Electromagnetic Calorimeter (ECAL) which contributes to the trigger, the  $e^+$ ,  $e^-$ ,  $\gamma$  identification and the energy as well as the charge via  $dE/dX$  measurements.

The maximal AMS acceptance given by the TRD and the inner Tracker, amounts to 0.5 m<sup>2</sup> str.

### 3 The Electromagnetic Calorimeter

The ECAL has three main purposes :

- To measure precisely the energy of electromagnetic particles up to the TeV range.

- To identify photons, electrons, positrons, so to be able to reject protons. Since the expected secondary positron flux is 1000 to 10000 lower than the one of protons, a rejection factor of at least  $1 \times 10^5$  is needed. This is achieved thanks to a high granularity in the longitudinal and lateral views.
- To trigger on photons thanks to a standalone ECAL trigger. In addition such redundant trigger is mandatory to increase the electron efficiency at high energy.

ECAL is a 3D imaging electromagnetic calorimeter, which consists of 9 modules (superlayers) made of a sandwich of grooved lead foils and of layers of scintillating fibers glued together representing an active area of  $648 \text{ mm} \times 648 \text{ mm}$  and a thickness of  $166.5 \text{ mm}$ . Each superlayer is  $18.5 \text{ mm}$  thick and made of 11 grooved (1 mm thick) lead foils interleaved with 10 layers of 1 mm diameter scintillating fibers. In each superlayer, the fibers run in one direction only and are alternatively read at one end by 4 anode PMTs. Each anode covers an active area of  $9 \text{ mm} \times 9 \text{ mm}$ , corresponding to 35 fibers, defined as a cell. In total the ECAL is subdivided into 1296 cells (324 PMTs). Thus the calorimeter consists of 18 longitudinal independent samplings leading to a segmentation in the longitudinal view (vertical axis) of 0.95 radiation length and in each lateral view ( $X$  and  $Y$ ) of 0.5 Moliere radius ( $R_M$ ). The ECAL acceptance amounts to  $0.06 \text{ m}^2 \text{ str}$ .

The longitudinal and lateral segmentation of the calorimeter allow a very high identification power for electromagnetic showers. In particular, the high longitudinal granularity enables to reconstruct the apex position (beginning of the shower) and then reject most of the protons ( $\sim 80\%$ ) starting an hadronic shower after the three first layers. The interaction length is of 28 layers (25.75 cm, or  $26.6X_0$ ). The calorimeter depth is then equivalent to  $0.64 \lambda_{\text{ind}}$ .

## 4 Analysis

The simplest method, known as rectangular cuts, consists in making individual simple cuts for each of the relevant variables. This method has limitation, because it does not take into account the correlations among the variables, and optimal cuts made on each variable are not guaranteed to give the optimal cuts for the whole of the variables. Overall, it allows to achieve a proton rejection factor ranging from 50 to 100 with an efficiency of 80-90%. This is not enough to reach the rejection goal even after having included the TRD and the tracker, maintaining an overall efficiency of 90%.

Thus the need to use a better optimization of the cuts by using more complex techniques, such as boosted decision trees or neural networks. We used the TMVA Package [2], and after comparisons between the techniques provided by the package, we chose to use the optimal one, *i.e.* boosted decision trees.

The implementation follows those steps :

1. We select two samples of events identified as signal and background.
2. We choose a set of relevant variables, which have individually proven to effectively discriminate between electron and proton.
3. The most discriminating variables are not necessarily the same for high and low energies ; we thus define

bins of different ranges in energy, on each of which the methods will be applied.

4. We run the boosted decision tree analysis on those sets ; it will give us an estimator, which allows us to quantify its identification power (in terms of efficiency / rejection), and a file of weights, which will allow us to carry the particles identification.
5. For each ISS event, the weight files will give us a number between 0 and 1 which, given the tests performed in previous steps, will allow us to quantify the probability of the event to be either hadronic or electromagnetic, and discriminate according to the rejection power needed.

## 5 Datasets

Due to the limitations of TRD identification, ECAL is the only subdetector really effective to identify particles at high energy. We used a sample of pure events selected both by TRD and  $E/p$  ratio, but mainly relied on identified data.

In August 2010, AMS-02 was tested with various beam tests (thereafter referred as BT) at Cern. Electrons of 100, 120, 180, and 300 GeV, and positrons of 10, 20, 80, 100, 120 and 180 GeV were used. A beam of 400 GeV hadrons was also used ; it served as our primary source of background. To have background above 400 GeV, we completed our sample with additional protons carefully selected using the TRD and  $E/p$  ratio.

One of our main goals was to have an estimator on a continuous range of energies up to several hundreds of GeV, which was not allowed solely by the points of energy for the signal. We completed our samples with a Monte-Carlo of simulated electrons (thereafter referred as MC) up to 595 GeV, by steps of 5 GeV, the statistics decreasing with energy from 1471000 events at 5 GeV, 207000 events at 100 GeV, 82000 at 300 GeV and 42000 at 595 GeV.

## 6 Variables

In the final version of the estimator, a total of 32 variables was used. they can merely be classified into three categories.

### 6.1 Shape-related variables

The variables correspond to classic indicators of the shape of an electromagnetic shower. The collimation of the shower, the number of layers before the apex (triggering of the shower, used to probe for minimum ionizing particles), footprint (transverse lateral profile surface), longitudinal and lateral dispersion are examples of such variables.

Figure 2 shows an example of such a variable.

### 6.2 Fit to the longitudinal electromagnetic shape

While a precise formula for an hadronic shower is hard to derive, most of the energy being not contained inside the detector, the development of an electromagnetic shower in the calorimeter is well-described by the formula :

$$\frac{dE}{dt_x} = E_0 \frac{b^{(\alpha+1)}}{\Gamma(\alpha+1)} t_x^\alpha e^{-bt_x} \quad (1)$$

where  $t_x = x/X_0$  is the normalized depth in units of radiation lengths  $X_0$ ,  $E_0$  is the energy of incident particle,  $\Gamma$  is the Euler gamma function, and  $b \approx 0.5$  allows us to retrieve  $\alpha$ .

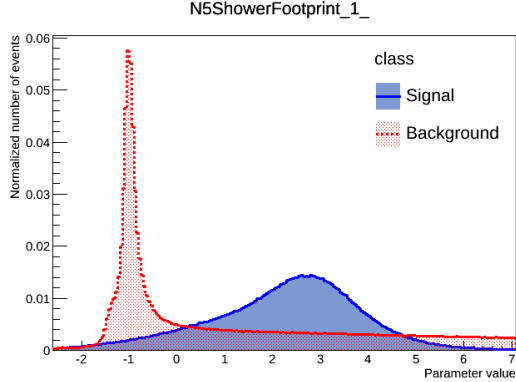


**Fig. 2:** Typical example of signal and background distributions for a variable (Shower Footprint)

Given a particular event, a certain number of variables were derived by estimating the matching between the event and the previous formula. We can quote the  $\chi^2$ , the computing of  $\alpha$ , an independent estimation for the  $b$  parameter (with a value greater than 0.5 for hadronic showers) from the energy of the shower and  $\alpha$  derived from the fit.

### 6.3 Energy-deposited variables

An electromagnetic shower is expected to deposit more energy than an hadronic one of same energy in the calorimeter, which brings more energy per cell, and less rear-leakage (fraction of energy not contained in the calorimeter).

In that purpose, we kept track of the ratios of energy deposited in the calorimeter to the number of pixels hit, total and only in the low gain channel (electromagnetic showers being supposed to deposit more energy in that channel), and of the square root of these number of pixels, for a total of four variables.

The rear leakage, ratio between deposited and reconstructed energy, is also calculated and used as a variable, as is its deviation from what would be expected from an electromagnetic shower.

## 7 Smearing

After the first training, tests were realized in order to assess the accuracy of our Ecal Standalone estimator (ESE). The signal was only trained on Monte-Carlo, which had proven to have differences with respect to real data. The estimator was tested against MC and BT for points having same energies. The results for 100 GeV are presented in Figure 3. The blue, plain curve shows the results from BT electrons, which was polluted by background. As we can see, the background peak is mixed with the protons peak (red, hatched), and the signal peak has the same value as the positron BT peak (black, hatched). However, there are huge differences with respect to the Monte-Carlo which is used as signal (green peak), and the two peaks are shifted towards background, jeopardizing the rejection values.

The next step was to check which of the variables exhibited differences between BT and MC. The Figure 4 shows, as an example, the distribution of the lateral distribution variable for beam test protons and electrons, and MC electrons. As we can see, the signal distribution for beam test is shifted towards the background.

All MC variables were examined, an a subsequent so-

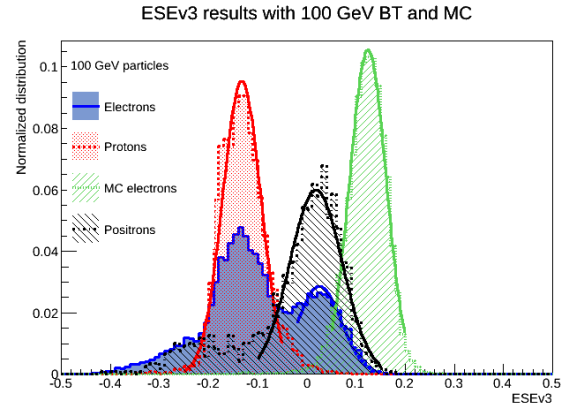


**Fig. 3:** Estimator results for MC electrons, and beam test protons, positrons and electrons at 100 GeV

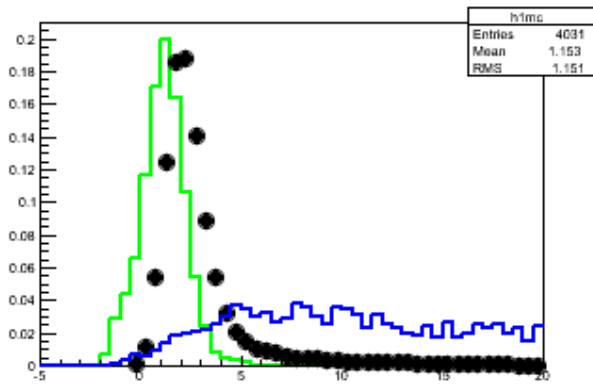


**Fig. 4:** Normalized distributions of lateral dispersion for BT protons (blue line), MC electrons (green line) and BT electrons (black points). The BT is shifted towards the background.

called *smearing* was applied on the relevant ones. This smearing, depending on the variables, could consist of :

- shift of the mean of each variable from the MC mean to the BT value;
- shift in mean with an additional gaussian noise added to account for greater  $\sigma$ .
- when the mean and  $\sigma$  had to be shifted with different values at different energies, the mean and  $\sigma$  values were computed for common energy points (namely 100, 120, 180 and 300 GeV), and interpolated/extrapolated to account for the whole energy range.

A visual check was made on all variables to ensure that the distributions matched before the smearing. The estimator was trained again with these smeared variables, using the procedure described above. The distributions for the same samples as before are shown in Figure 5. As we can see, after the smearing of the input variables, the signal peaks for simulations and actual variables are in the same position. The further tests on the quality of the estimator can be processed.

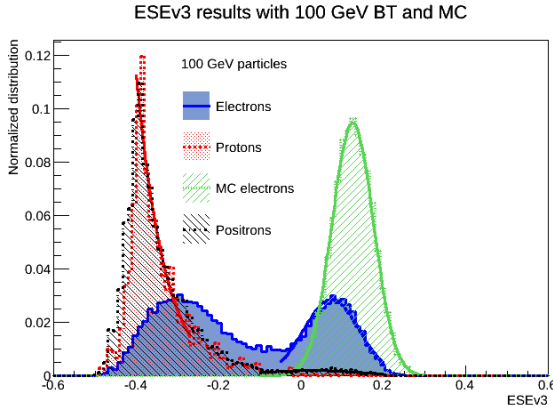


**Fig. 5:** Estimator results at 100 GeV after smearing. The signal peaks are at the same position. A contamination is visible in the BT electrons.

## 8 Overfitting checks

An important feature to be checked for before assessing rejection values is the overfitting. This effect occurs when an excessively complex model (typically, with two many variables with respect to the size of samples) leads to a description of noise instead of the underlying relationships between the variables.

The training of the estimator uses only half of the available events (the training sample), and the remaining half (the test sample) is used to test the power of the estimator on a similar statistics. Figure 6 shows the distribution of the estimator for the two samples. As we can see, the two distributions are very similar, which is a strong indication of the absence of overfitting (in case of overfitting, they wouldn't match).

The quantification of this matching is classically done through a Kolmogorov-Smirnov test. The probability of this test on our distributions is of a 90.6% likelihood. That score indicates a good compatibility between the samples and confirms the absence of overfitting of our data.

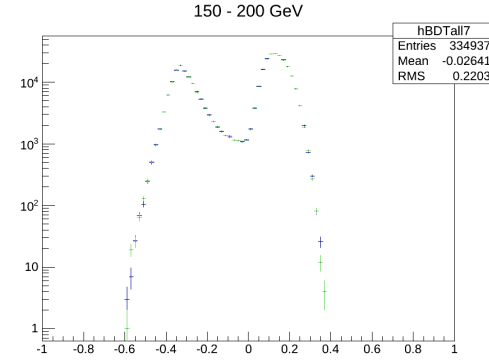


**Fig. 6:** Overfitting checks for ESEv3. The two curves match, indicating no evidence of overfitting.

## 9 Final proton rejection

The final proton rejection is ultimately computed. For each bin, and keeping an efficiency of 90% of the electrons, the rejection is defined as the inverse of the fraction of protons of the test sample passing through the estimator. In our case, we expect at least a rejection of 1000 to match the objectives stated before. The results are shown in Figure 7.

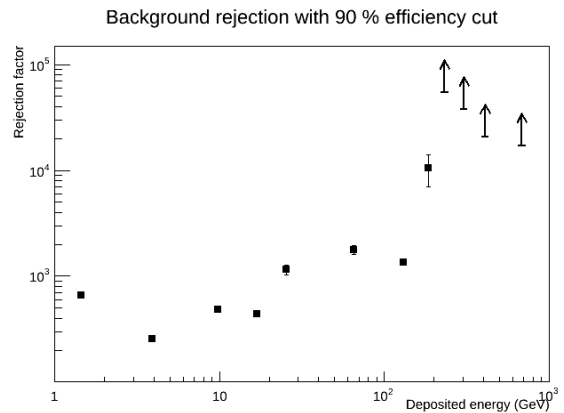


**Fig. 7:** Final rejection values of our estimator for a 90% efficiency.

For the highest energies, no protons of the test sample passed the cuts of the 90% efficiency, which allows us only to give a minimum value for the rejection factor. At the end, the proton rejection goes from a few hundreds below 10 GeV to more than  $2 \times 10^4$  above 300 GeV.

Combined with the other detectors (TRD and Energy and momentum from the tracker matching) an overall rejection factor of  $1 \times 10^6$  is achieved, from 2 GeV to more than 100 GeV. The estimator fulfills its role.

## 10 Conclusions

The protons rejection is primordial in order to compute the positrons ratios. Using the features of the electromagnetic calorimeter of the AMS02 experiment, we built an estimator allowing to reject with efficiency this background. The background test consisted mainly of a beam test of hadrons, while the signal was obtained through simulations, whose variables had to be smeared to meet the distributions of actual particles. No sign of overfitting was observed.

For a 90% electron efficiency, we obtain a rejection factor of more than  $10^4$  above 100 GeV, meeting the expectancy of the detector at high energies.

## References

- [1] Rosier-Lees, Sylvie, on behalf of the AMS02 collaboration. "Performance of the AMS02 Electromagnetic Calorimeter in Space." *Journal of Physics: Conference Series* 404 (December 21, 2012): 012034. doi:10.1088/1742-6596/404/1/012034.
- [2] Hoecker, A. et al. "TMVA - Toolkit for Multivariate Data Analysis." *arXiv:physics/0703039* (March 4, 2007).